



## Model MTF for the mosaic window

Zhenchong Xing, Yongfeng Hong & Bao Zhang

To cite this article: Zhenchong Xing, Yongfeng Hong & Bao Zhang (2017) Model MTF for the mosaic window, Journal of Modern Optics, 64:19, 2074-2082, DOI: [10.1080/09500340.2017.1337940](https://doi.org/10.1080/09500340.2017.1337940)

To link to this article: <http://dx.doi.org/10.1080/09500340.2017.1337940>



Published online: 12 Jun 2017.



Submit your article to this journal [↗](#)



Article views: 5



View related articles [↗](#)



View Crossmark data [↗](#)



## Model MTF for the mosaic window

Zhenchong Xing, Yongfeng Hong and Bao Zhang

Changchun Institute of Optics Fine Mechanics and Physics, Chinese Academy of Science, Changchun, China

### ABSTRACT

An electro-optical targeting system mounted either within an airframe or housed in separate pods requires a window to form an environmental barrier to the outside world. In current practice, such windows usually use a mosaic or segmented window. When scanning the target, internally gimbaled systems sweep over the window, which can affect the modulation transfer function (MTF) due to wave-front division and optical path differences arising from the thickness/wedge differences between panes. In this paper, a mathematical model of the MTF of the mosaic window is presented that allows an analysis of influencing factors; we show how the model may be integrated into ZEMAX® software for optical design. The model can be used to guide both the design and the tolerance analysis of optical systems that employ a mosaic window.

### ARTICLE HISTORY

Received 22 October 2016  
Accepted 25 May 2017

### KEYWORDS

Imaging systems; optical window; modulation transfer function; diffractive optics

## 1. Introduction

A mosaic window is widely used to achieve both stealth and better aerodynamic performance in military applications that employ conformal optics. Many published studies have analysed mosaic windows, with research interest mainly focused on the effect of mosaic windows on the MTF of optical systems [1–6]. In particular, the influence of the incidence angle on the optical path difference (OPD), and hence on the MTF is of importance when the wave-fronts are split into two or two equal parts by the window. In this paper, we address these complex situations and how one may carry out the corresponding mathematical calculation of the MTF.

## 2. Optical configurations

The optical window of the electro-optical targeting system (EOTS) of F-35 is the most typical representative of the conformal mosaic window, which is illustrated in Figure 1. [7,8] The window consists of multiple flat panes. The imaging system turns around its axis inside a fixed structure possessing several pieces of window panes [3], such as Figure 2.

For some scanning angles, the wave-front incident at the window has to pass through several panes simultaneously. When the system is directed at an angle  $\alpha$ , shown as Figure 3, the angle between the two panes is  $\pi - A$  and the two parts of the wave-front arrive at the two panes

at angles  $\alpha$  and  $A - \alpha$  respectively. When  $\alpha \neq A/2$ , the two angles are not equal, which will lead to the difference of the angles at which the light propagates inside the window panes and will give rise to unequal optical path length (OPL), even if the thickness of window panes are same [3].

When the wave-front is equally divided into two parts by the window, as shown in Figure 3,  $\alpha$  and  $A - \alpha$  are the incidence angles at the two window panes.  $\theta_1$  and  $\theta_2$  are refraction angles inside the window.  $n$  is the refractive index of the window and  $d$  is the thickness [2]. The  $f$  indicates the focal length of the optical system.  $D_1$  and  $D_2$  are the OPL in the upper pane and the OPL in the lower pane.  $\Delta D$  is the difference between the upper OPL and lower OPL.  $\Delta\varphi$  is the phase difference caused by the  $\Delta D$ .  $\lambda$  is the wavelength of the monochromatic light. The formulas of these parameters are shown as Equations (1)–(4) [3]:

$$\Delta D = D_1 - D_2 = nd / \cos(\theta_1) - nd / \cos(\theta_2) \quad (1)$$

$$n \sin(\theta_1) = \sin(\alpha) \quad (2)$$

$$n \sin(\theta_2) = \sin(A - \alpha) \quad (3)$$

$$\Delta\varphi = 2\pi\Delta D / \lambda \quad (4)$$

when  $\alpha = A/2$ , but the panes of the window are not of the same thickness, the OPD will be created. As shown in Figure 4,  $D_1$  is the OPL at the upper pane. The lower pane

has a wedge angle  $\gamma$ , which gives rise to the problem of aliasing image.  $\delta$  is the deflective angle of the lower light beam.  $\Delta y$  is the offset of the lower image point.  $D$  is the diameter of the pupil.  $\delta$  and  $\Delta y$  are shown in Equations (5) and (6).

$$\delta = \gamma(n - 1) \tag{5}$$

$$\Delta y = f \tan(\delta) \tag{6}$$

Because of the wedge angle, the OPL and the phase difference is a function of  $y$  based on Figure 4. The  $\Delta D$  and  $\Delta\varphi$  can be formulated in Equations (9) and (10).

$$D_1 = dn \tag{7}$$

$$D_2 = (d + y \tan(\gamma))n \tag{8}$$

$$\Delta D = D_2 - D_1 = y(n - 1) \tan(\gamma) \tag{9}$$

$$\Delta\varphi = 2\pi(n - 1)\left(\frac{D}{2} - y\right) \tan(\gamma)/\lambda \tag{10}$$

As previously described, the incident angle of the wave-front and the wedge angle of the window pane can cause wave-front division and the phase difference between the parts of the wave-front. It is these differences that give rise to the change of the MTF.

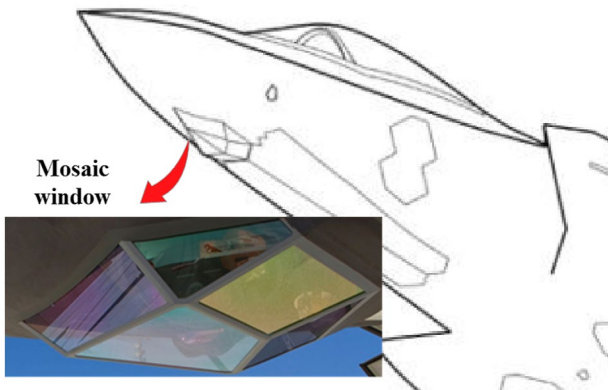


Figure 1. Conformal optical window of EOTS.

### 3. Theoretical analysis

#### 3.1. Theoretical formula of OTF

MTF is the important indicator of imaging optical systems. To further understanding of the effect of the mosaic window on the MTF, we need to know the mathematical model of the optical transfer function (OTF). OTF can be expressed in Equation (11).

$$\text{OTF}(f_x, f_y) = m(f_x, f_y) \exp \left[ i\varphi(f_x, f_y) \right] \tag{11}$$

Among the Equation (11),  $m(f_x, f_y)$  is the MTF.  $\varphi(f_x, f_y)$  is the phase transfer function. MTF is the modulus of the monochromatic OTF. Thus, assume diffraction-limited optics centred on the split in a mosaic window, the MTF in the meridional direction that is showed in Figures 3 and 4 is expressed as Equation (12) [3].

$$\begin{aligned} \text{MTF}(f_x, f_y) &= \left| \text{OTF}(f_x, f_y) \right| = \left| \frac{P(f_x, f_y) \otimes P(f_x, f_y)}{\iint_{-\infty}^{\infty} |P(\xi, \eta)|^2 d\xi d\eta} \right| \\ &= \left| \frac{\iint_{-\infty}^{\infty} P(\xi, \eta) \cdot P^*(\xi - f_x, \eta - f_y) d\xi d\eta}{\iint_{-\infty}^{\infty} |P(\xi, \eta)|^2 d\xi d\eta} \right| \end{aligned} \tag{12}$$

$\otimes$  is the auto-correlation.  $P(f_x, f_y)$  is the pupil function. According to the theory of the auto-correlation, the computation process of MTF is the process to calculating overlapping area of the normalized pupil function. According to the Equation (12), the pupil function is the

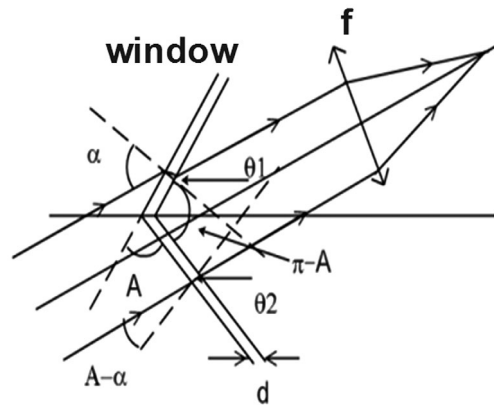


Figure 3. Geometry of system aperture facing two window panes.

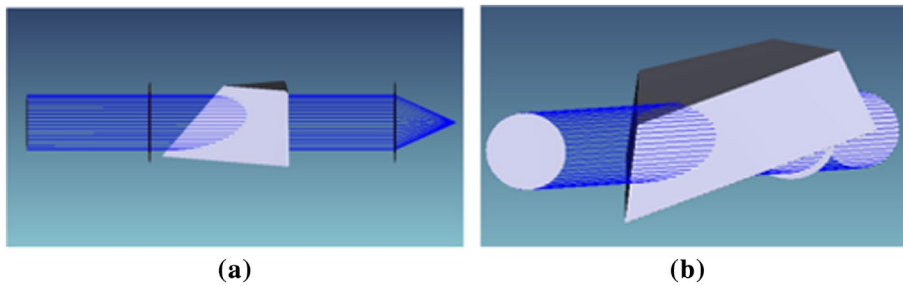
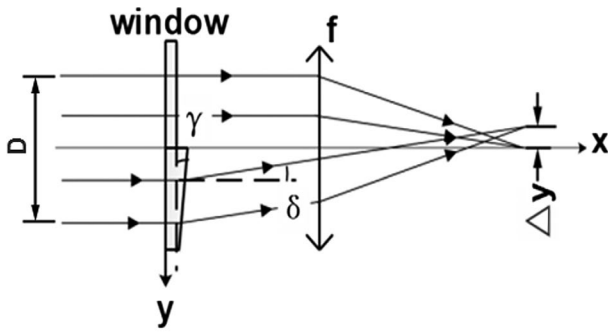
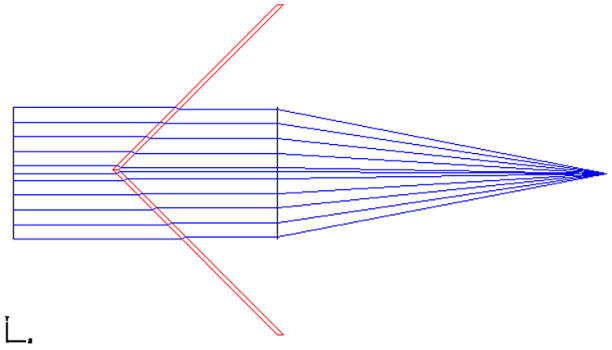


Figure 2. Optical system to target possessing different places of window: (a) system aperture faces with two panes of the window, (b) system aperture faces with three panes of the window.



**Figure 4.** System aperture facing the window panes with wedge angle.



**Figure 5.** System aperture faces with two equal panes when  $\alpha = A/2$ .

main influence of the MTF. The later calculations are based on the above theory model to find mathematic relation between the main impact factors and the MTF.

### 3.2. Simulation with static turbulence

With the rotation of the system, the pupil function is ever changing, so is MTF.

#### 3.2.1. The calculation for the OTF in a special situation

When the wave-front is equally divided into two parts by the window as shown in Figure 5, the analysis of the effects in the monochromatic system was given by Gimlet [2].

The phases of the wave-fronts are  $\varphi_1$  and  $\varphi_2$ . So, the phase difference is shown as Equation (4) and the pupil function is expressed in Equation (13). The  $f_x$  and  $f_y$  are the spatial frequencies.

$$P(f_x, f_y) = \begin{cases} e^{i\varphi_1} & f_x^2 + f_y^2 \leq f_0^2, f_x < 0 \\ e^{i\varphi_2} & f_x^2 + f_y^2 \leq f_0^2, f_x \geq 0 \\ 0 & f_x^2 + f_y^2 > f_0^2 \end{cases} \quad (13)$$

$f_0$  ( $f_0 = 1/2\lambda F$ ) indicates the coherent cut-off frequency and  $F$  is the  $F$ -number of the system.

We can obtain the OTF shown as in Equation (14) by substituting the Equation (13) into the Equation (12). Figure 6 is the pupil function convolution.

$$OTF(f_x, 0) = \begin{cases} M_0(2f_x) + [M_0(f_x) - M(2f_x)] \exp(i(\varphi_2 - \varphi_1)) & 0 \leq |f_x/2f_0| \leq 1/2 \\ M_0(f_x) \exp(i(\varphi_2 - \varphi_1)) & 1/2 \leq |f_x/2f_0| \leq 1 \\ 0 & |f_x/2f_0| > 1 \end{cases} \quad (14)$$

where  $M_0(f_x)$  is the MTF of a monochromatic perfect lens and it is formulated in Equation (15):

$$M_0(f_x) = \frac{2}{\pi} \left\{ \cos^{-1} \left( \frac{f_x}{2f_0} \right) - \frac{f_x}{2f_0} \sqrt{1 - \left( \frac{f_x}{2f_0} \right)^2} \right\} \quad f_x \leq 2f_0 \quad (15)$$

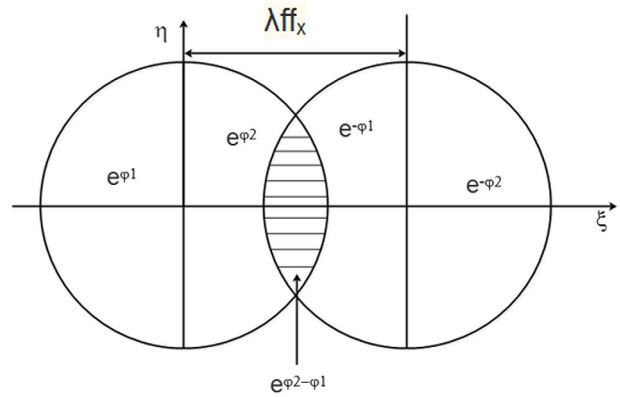


**Figure 6.** Pupil function convolution when wave-front is equally divided into two parts.

#### 3.2.2. The calculation for the OTF in a common situation

Nevertheless, when the system continues turning, the wave-front will be unequally divided into two parts by the window as shown in Figure 3. Figure 3 can indicate that the rotation of the system gives rise to the changes of the position of the septa and incidence angle.

Figure 7 is the corresponding pupil function convolution, where  $D$  is the pupil diameter and  $\sigma$  is the ratio of the rise of left part of the pupil to the pupil diameter.

It is further suggested that the changes of the position of the septa and incidence angle cause the changes of the phase difference and formula of the pupil function, by the Figure 7. So, the OTF is affected by the  $\sigma$  and  $\Delta\varphi$ .

For conciseness, we define  $f_n = (1 - \frac{2}{\sigma})f_0$ . When  $\sigma > 3$ , the OTF can be expressed as Equation (16):

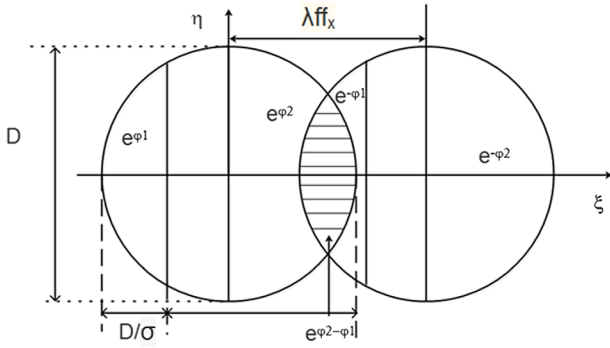


Figure 7. Pupil function convolution when  $a \neq A/2$ .

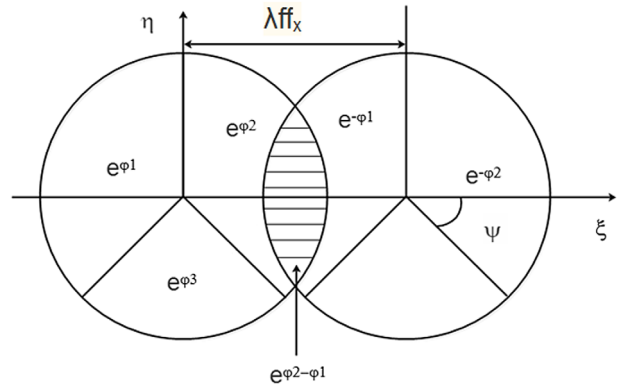


Figure 8. Pupil function convolution when  $\psi = 30^\circ$ .

$$\text{OTF}(f_x, 0) = \begin{cases} \frac{M_0(2(f_n+f_x))}{2} + \left(\frac{M_0(2f_n)}{2} - \frac{M_0(2(f_n+f_x))}{2}\right)e^{i(\varphi_2-\varphi_1)} + \dots M_0(f_x) - \frac{M_0(2f_n)}{2} & 0 \leq f_x \leq \frac{2}{\sigma} \\ \frac{M_0(2(f_n))}{2} e^{i(\varphi_2-\varphi_1)} + \left(M_0(f_x) - \frac{M_0(2f_n)}{2}\right) & \frac{2}{\sigma} \leq f_x \leq \left(2 - \frac{4}{\sigma}\right)f_0 \\ \left(M_0(f_x) - \frac{M_0(2(f_x-f_n))}{2}\right)e^{i(\varphi_2-\varphi_1)} + \frac{M_0(2(f_x-f_n))}{2} & \left(2 - \frac{4}{\sigma}\right)f_0 \leq f_x \leq \left(1 - \frac{1}{\sigma}\right)2f_0 \\ M_0(f_x)e^{i(\varphi_2-\varphi_1)} & \left(1 - \frac{1}{\sigma}\right)2f_0 \leq f_x \leq 2f_0 \\ 0 & f_x > 2f_0 \end{cases} \quad (16)$$

when  $\sigma \leq 3$ , the OTF can be expressed as Equation (17). When  $\sigma = 2$ , Equation (17) can be simplified to Equation (14).

$$\text{OTF}(f_x, 0) = \begin{cases} \frac{M_0(2(f_n+f_x))}{2} + \left(\frac{M_0(2f_n)}{2} - \frac{M_0(2(f_n+f_x))}{2}\right)e^{i(\varphi_2-\varphi_1)} + M_0(f_x) - \frac{M_0(2f_n)}{2} & 0 \leq f_x \leq \left(1 - \frac{2}{\sigma}\right)f_0 \\ \frac{M_0(2(f_n+f_x))}{2} + \frac{M_0(2(f_x-f_n))}{2} + \left(M_0(f_x) - \frac{M_0(2(f_x-f_n))}{2} - \dots \frac{M_0(2(f_n+f_x))}{2}\right)e^{i(\varphi_2-\varphi_1)} & \left(1 - \frac{2}{\sigma}\right)f_0 \leq f_x \leq \frac{2}{\sigma}f_0 \\ \frac{M_0(2(f_n+f_x))}{2} + \left(M_0(f_x) - \frac{M_0(2(f_n+f_x))}{2}\right)e^{i(\varphi_2-\varphi_1)} & \frac{2}{\sigma}f_0 \leq f_x \leq \left(2 - \frac{2}{\sigma}\right)f_0 \\ M_0(f_x)e^{i(\varphi_2-\varphi_1)} & \left(1 - \frac{1}{\sigma}\right)2f_0 \leq f_x \leq 2f_0 \\ 0 & f_x > 2f_0 \end{cases} \quad (17)$$

In more complex cases, the wave-front is split into three equal parts, such as Figures 2(b) and 8 is the corresponding pupil function convolution. The fan angle of the pupil is  $\psi + \pi/2$  in Figure 8.

For conciseness, we define  $\beta_1 = \arccos\left(\frac{f_x}{f_0} \sin\psi\right)$  and  $\beta_2 = \psi - \beta_1$ . The OTF may be expressed in terms of the  $M_0(f_x)$ ,  $\beta_1$  and  $\beta_2$  as Equation (18):

$$\text{OTF}(f_x, 0) = \begin{cases} \left(\frac{M_0(f_x)}{2} - \frac{M_0(2f_x)}{2}\right)e^{i(\varphi_2-\varphi_1)} + \left(\frac{M_0(2f_x)}{2} + \frac{\beta_2}{\pi} - \frac{\sin(\beta_2)}{\pi} \left(\frac{f_x}{f_0}\right)\right) + \frac{\tan(\psi)}{\pi} \left(\frac{f_x}{2f_0}\right)^2 e^{i(\varphi_2-\varphi_1)} \\ + \left(\frac{\psi}{2\pi} - \left(\frac{\beta_1}{2\pi} + \frac{\sin(\psi-\beta_1)}{2\pi} \left(\frac{f_x}{f_0}\right)\right) - \frac{\tan(\psi)}{\pi} \left(\frac{f_x}{2f_0}\right)^2\right) (e^{i(\varphi_3-\varphi_1)} + e^{i(\varphi_2-\varphi_3)}) \dots \\ + \left(\frac{M_0(f_x)}{2} - \frac{\psi}{\pi} + \frac{\tan(\psi)}{\pi} \left(\frac{f_x}{2f_0}\right)^2\right) & 0 \leq f_x \leq f_0 \\ \frac{M_0(f_x)}{2} e^{i(\varphi_2-\varphi_1)} + \frac{f_x \tan(K)(2f_0-f_x)}{4\pi f_0^2} e^{i(\varphi_2-\varphi_1)} + \left(\frac{\psi}{2\pi} - \frac{f_x \tan(K)(2f_0-f_x)}{4\pi f_0^2}\right) e^{i(\varphi_3-\varphi_1)} \dots \\ + \left(\frac{\psi}{2\pi} - \frac{f_x \tan(K)(2f_0-f_x)}{4\pi f_0^2}\right) e^{i(\varphi_2-\varphi_3)} + \left(\frac{M_0(f_x)}{2} - \frac{\psi}{\pi} + \frac{1}{\pi} \tan(\psi) \frac{f_x^2}{4f_0^2}\right) & f_0 \leq f_x \leq \sqrt{3}f_0 \\ M_0(f_x)e^{i(\varphi_2-\varphi_1)} & \sqrt{3}f_0 \leq f_x \leq 2f_0 \\ 0 & f_x > 2f_0 \end{cases} \quad (18)$$

If assuming the same incidence angle, the following calculations will refer only to OPDs due to the wedge angle of the window, as shown in Figure 4.

The phase difference in this condition is as shown in Equation (10). So, the pupil function can be shown in Equation (19).

$$P(f'_x, f'_y) = \begin{cases} e^{2\pi(n-1)(\frac{D}{2} + \xi) \tan(\gamma)/\lambda} = e^{i2(n-1)\pi f(f_0 + f_x) \tan \gamma} & f_x^2 + f_y^2 \leq f_0^2, f_x < 0 \\ 1 & f_x^2 + f_y^2 \leq f_0^2, f_x \geq 0 \\ 0 & f_x^2 + f_y^2 \geq f_0^2 \end{cases} \quad (19)$$

We can substitute Equation (19) into Equation (12) to obtain the OTF shown in Equation (20).

$$\begin{cases} \frac{M_0(2f_x)}{2} + \frac{M_0(2f_x)}{2} e^{i2\pi(n-1) \tan \gamma f f_x} + 2 \left( \int_{-\lambda f f_x/2}^{-\lambda f f_x/2} \sqrt{R^2 - x^2} e^{i\frac{2\pi}{\lambda}(n-1) \tan \gamma(R+x)} dx \dots \right. \\ \left. + \int_{-\lambda f f_x/2}^0 \sqrt{R^2 - (a+x)^2} e^{i\frac{2\pi}{\lambda}(n-1) \tan \gamma(R+x)} dx \right) & 0 \leq |f_x/2f_0| \leq 1/2 \\ 2 \left( \int_{-D/2}^{-\lambda f f_x/2} \sqrt{R^2 - x^2} e^{-i\frac{2\pi}{\lambda}(n-1) \tan \gamma(R+x)} dx + \int_{-\lambda f f_x/2}^{D/2 - \lambda f f_x} \sqrt{R^2 - (a+x)^2} e^{-i\frac{2\pi}{\lambda}(n-1) \tan \gamma(R+x)} dx \right) & 1/2 \leq |f_x/2f_0| \leq 1 \\ 0 & |f_x/2f_0| > 1 \end{cases} \quad (20)$$

### 3.3. Polychromatic OTF for a mosaic window

In practice, we need study on the MTF in the polychromatic case. As mentioned above, when the panes of the window are not of the same thickness, OTF includes a phase shift of  $e^{i\frac{2\pi}{\lambda} \Delta D}$ , which is depending on  $\lambda$ . In the case of polychromatic illumination, the OTF must be averaged including this phase shift. According to the research result of Dov Freiman, Menachem Nadler and Yuval Gronau, the

$$C_1 = \cos^{-1} \left( 1 - \frac{2}{\sigma} + \frac{f_x}{f_0} \right) \quad (21)$$

$$C_2 = \cos^{-1} \left( 1 - \frac{2}{\sigma} \right) \quad (22)$$

$$C_3 = \cos^{-1} \left( \frac{f_x}{f_0} + \frac{2}{\sigma} - 1 \right) \quad (23)$$

$$\text{OTF}(f_x, 0) = \begin{cases} 2 \left( \frac{C_1}{2\pi} - \frac{1}{2\pi} \frac{\cos C_1}{\sin \beta_1} \right) + \left( M_0(f_x) - 2 \left( \frac{C_2}{2\pi} - \frac{1}{2\pi} \frac{\cos C_2}{\sin C_2} \right) \right) & 0 \leq f_x \leq \frac{2}{\sigma} f_0 \\ \left( M_0(f_x) - 2 \left( \frac{C_2}{2\pi} - \frac{1}{2\pi} \frac{\cos C_2}{\sin C_2} \right) \right) & \frac{2}{\sigma} f_0 \leq f_x \leq \left( 2 - \frac{4}{\sigma} \right) f_0 \\ 2 \left( \frac{C_3}{2\pi} - \frac{\tan(C_3)}{2\pi} \left( \frac{f_x}{f_0} + \frac{2}{\sigma} - 1 \right)^2 \right) & \left( 2 - \frac{4}{\sigma} \right) f_0 \leq f_x \leq \left( 1 - \frac{1}{\sigma} \right) 2f_0 \\ 0 & f_x > \left( 1 - \frac{1}{\sigma} \right) 2f_0 \end{cases} \quad (24)$$

when  $\sigma < 3$ , the OTF can be shown in Equation (25).

$$\text{OTF}(f_x, 0) = \begin{cases} 2 \left( \frac{C_1}{2\pi} - \frac{1}{2\pi} \frac{\cos C_1}{\sin C_1} \right) + \left( M_0(f_x) - 2 \left( \frac{C_2}{2\pi} - \frac{1}{2\pi} \frac{\cos C_2}{\sin C_2} \right) \right) & 0 \leq f_x \leq \left( 1 - \frac{2}{\sigma} \right) f_0 \\ 2 \left( \frac{C_1}{2\pi} - \frac{1}{2\pi} \frac{\cos C_1}{\sin \beta_1} \right) + 2 \left( \frac{C_3}{2\pi} - \frac{1}{2\pi} \frac{\cos C_3}{\sin C_3} \right) & \left( 1 - \frac{2}{\sigma} \right) f_0 \leq f_x \leq \frac{2}{\sigma} f_0 \\ 2 \left( \frac{C_3}{2\pi} - \frac{1}{2\pi} \frac{\cos C_3}{\sin C_3} \right) & \frac{2}{\sigma} f_0 \leq f_x \leq \left( 2 - \frac{2}{\sigma} \right) f_0 \\ 0 & f_x > \left( 2 - \frac{2}{\sigma} \right) f_0 \end{cases} \quad (25)$$

phase difference  $\Delta\phi$  covers all the values between 0 and  $2\pi$  uniformly. When the OTF is averaged over all wavelengths, the expressions that include  $e^{i\Delta\phi}$  are averaged to zero. [3] So we can get the OTF in the polychromatic case. For conciseness, we define the Equation (21)–(23). When the wave-front is equally divided into two parts and  $\sigma \geq 3$ , the OTF can be shown in Equation (24).

Based on the Equations (24) and (25), when the thickness of panes of the window is same, the OTF in the case of polychromatic illumination is unaffected except by the position of the septa. The position of the septa is in flux and  $\sigma$  is ever changing. The MTF is the function with the  $\sigma$  variable. Figure 9 shows the change of the MTF with the  $n$ , according to the Equations (24) and (25).

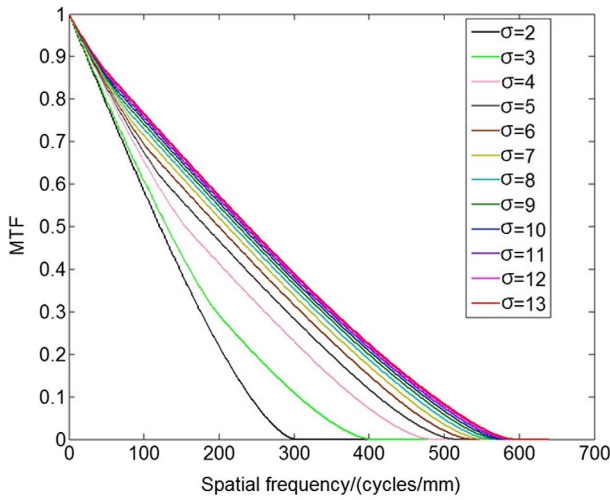


Figure 9. The MTF varies with the  $\sigma$ .

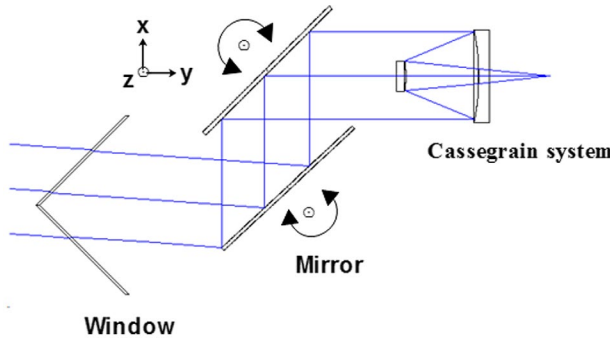


Figure 10. The model of the optical system aperture facing two panes.

When the wave-front is equally divided into three equal parts in the polychromatic case, the OTF can be shown in Equation (26):

$$OTF(f_x, 0) = \begin{cases} \left( \frac{\beta_2}{2\pi} + \frac{\sin(\psi - \beta_2)}{2\pi} \left( \frac{f_x}{f_0} \right) + \left( \frac{M_0(f_x)}{2} - \frac{\psi}{\pi} + \frac{\tan(\psi)}{\pi} \left( \frac{f_x}{2f_0} \right)^2 \right) \right) & 0 \leq f_x \leq f_0 \\ \frac{M_0(f_x)}{2} - \frac{\psi}{\pi} + \frac{1}{\pi} \tan(\psi) \frac{f_x^2}{4f_0^2} & f_0 \leq f_x \leq \sqrt{3}f_0 \\ 0 & \sqrt{3}f_0 \leq f_x \end{cases} \quad (26)$$

### 3.4. Cascaded mosaic window MTF for a Cassegrain reflector

The model MTF of the mosaic window can be extended to a more realistic configuration of the EOTS that includes Cassegrain reflector optics. Figure 10 shows that the gimbaled system can sweep over the window.

When scanning the target, the MTF at the Nyquist frequency will be decreased. The MTF of the Cassegrain system is denoted by  $MTF_c$ . The MTF of the window is denoted by  $MTF_\sigma$ .  $MTF_{cw}$  is the MTF of the Cassegrain system with the mosaic window.

$$MTF_{cw} = MTF_c \times MTF_\sigma \quad (27)$$

## 4. Simulation set-up

A simulation of the degradation effect caused by the position of the septa and different phases at the mosaic window is performed by using the ZEMAX software to verify the correctness of the obtained MTF formulas. The mosaic window is modelled in ZEMAX by using the function of non-sequential component (NSC) with ports and defining polygon objects. Figure 2 simulates the situation that an optical system faces the mosaic window. To avoid the optical system to be affected by the MTF, the optical system is a paraxial lens and its focal length is 100 mm. The diameter of the aperture is 32 mm. The wavelength of the monochromatic light is 0.5  $\mu\text{m}$ . The wavelength range of the Polychromatic light is 0.45–0.65  $\mu\text{m}$ . By setting the parameters to rotating the optical system, the model can simulate that the system aperture faces window with two panes in different directions shown in Figure 11. It is the changes in the position of the septa and the OPD that cause the changes in the MTF when the system aperture faces with two equal thickness panes. The panes tilted with respect to each other shown in Figure 2 can be equivalent to a pane divided into several parts with different thickness. By changing the thicknesses of the panes and the position of the septa, the model shown in Figures 11(b) and 12 can simulate the case shown in Figure 2(a) and the case shown in Figure 2(b), which can simplify the computational process of the ZEMAX. Similarly, when considering the wedge angle only, the window can be simplified to the model shown in the Figure 13. Based on the simulation model, the theoretic results are well tested.

## 5. Results

In order to verify the formulas of the situation that the system aperture faces two window panes with same thickness, the model of Figure 11 is used. With rotating the optical system, the  $\sigma$  is changing, such as Figure 7. We choose some random positions. To save some space, Table 1 only presents the monochromatic diffraction MTF for  $\sigma = 3$  and  $\sigma = 4$  and the monochromatic diffraction MTF calculated by Equations (16) and (17) in the same conditions. The calculating results tally with the simulation results.

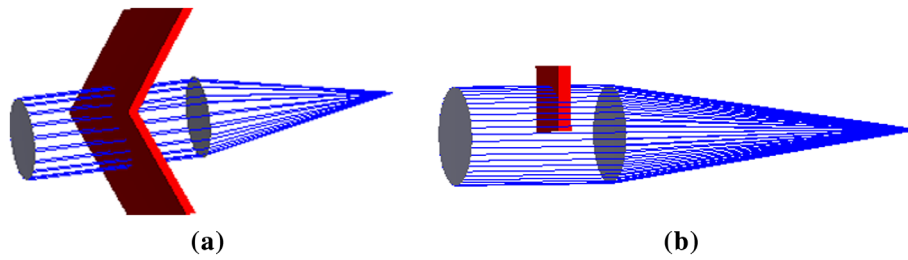


**Figure 11.** The model of system aperture facing two panes: (a) the window model with two panes in different directions model, (b) simplified model.

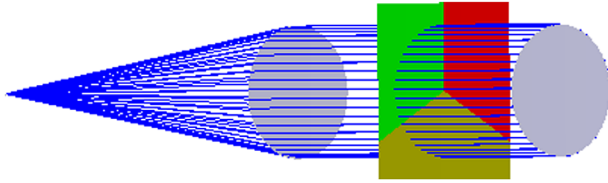


**Figure 12.** The simplified model of system aperture facing three panes.

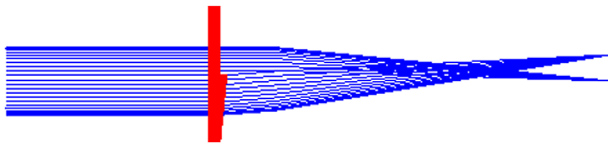


**Figure 13.** The simplified model of system aperture facing the window with the wedge angle.

In order to verify the formulas of the situation that the system aperture faces, three equal window panes, the model of Figure 12 is used. The different phases are achieved by applying different optical thicknesses to the three glass plates. Table 2 presents the monochromatic diffraction MTF for phase of  $\varphi_1 = 0, \varphi_2 = 0.2488\pi, \varphi_3 = 0.74664\pi$  and the monochromatic diffraction MTF for phase of  $\varphi_1 = 0, \varphi_2 = 0.5205\pi, \varphi_3 = 1.003588\pi$  and the corresponding monochromatic diffraction MTF calculated by Equation (18) in the same conditions. The calculating results tally with the simulation results.

In order to verify the formulas of the situation that the system aperture faces two window panes, one of which has a wedge angle, the model of Figure 13 is used. The different phases are achieved by applying different forms to the two glass panes. One of the panes has a wedge angle  $\gamma$ , which can be changed by using defining polygon objects utility of ZEMAX. Table 3 presents the monochromatic diffraction MTF for  $\gamma$  of  $0.000286^\circ$  and  $0.0286^\circ$  and the monochromatic diffraction MTF calculated by Equations (19) and (20) in the same conditions. The calculating results tally with the simulation results.

In order to verify the formulas of the situation that the system aperture faces two window panes in the polychromatic case, the model of Figure 11 is used. With rotating the optical system, the  $\sigma$  is changing such as Figure 7. We choose some random positions. Table 4 presents the polychromatic diffraction MTF for  $\sigma = 2$  and  $\sigma = 3$  in the polychromatic case and the polychromatic diffraction MTF calculated by Equations (16) and (17) in the same conditions. The calculated results tally with the simulation results.

According to the above results, we can calculate mosaic window MTF for a Cassegrain reflector. When the size of CCD pixel is  $7.5 \mu\text{m}$ , and the fields of the Cassegrain system are  $0^\circ$ (field 1),  $0.2^\circ$ (field 2), and  $-0.2^\circ$ (field 3). For example, when  $\sigma = 3$ ,  $\text{MTF}_\sigma$  is denoted by  $\text{MTF}_{\sigma=3}$ . Figure 14 shows the MTF of the Cassegrain system, and Figure 15 shows  $\text{MTF}_{c_w}$  with  $\sigma = 3$ . On the basis of Figure 9, the range of variation of the  $\text{MTF}_\sigma$  is 0.55–0.85. If design requests  $\text{MTF}_{c_w}$  at the Nyquist frequency is greater than

**Table 1.** The comparison of ZEMAX MTF and Model MTF when the system faces two equal window panes in different conditions.

Condition	$\sigma = 3$	$\sigma = 4$
MTF		

**Table 2.** ZEMAX MTF results when the system faces three equal window panes.

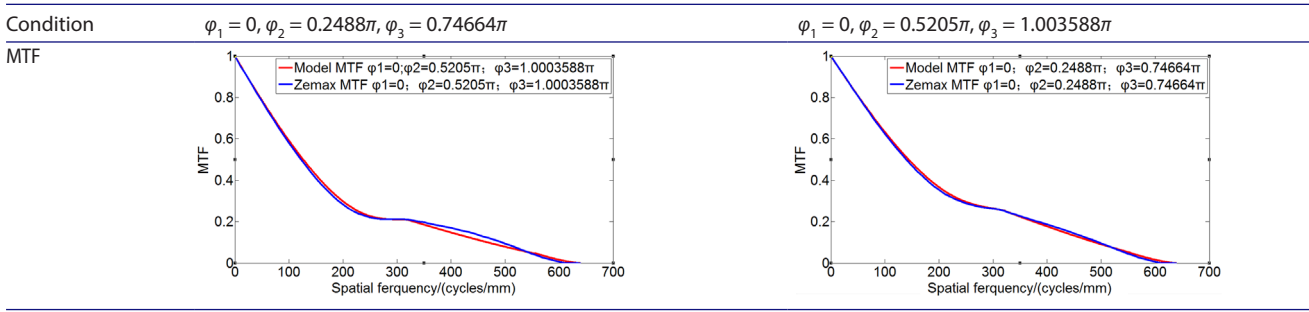


**Table 3.** The comparison of ZEMAX MTF and Model MTF when the pane has a wedge angle in different conditions.

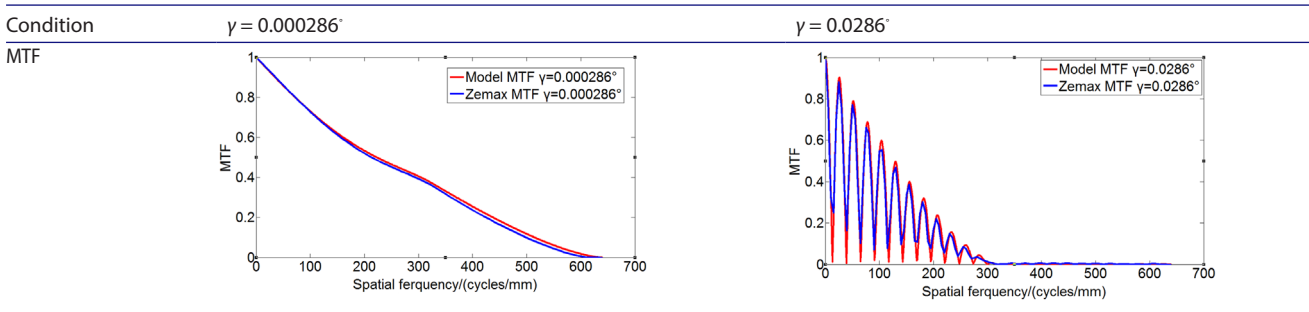
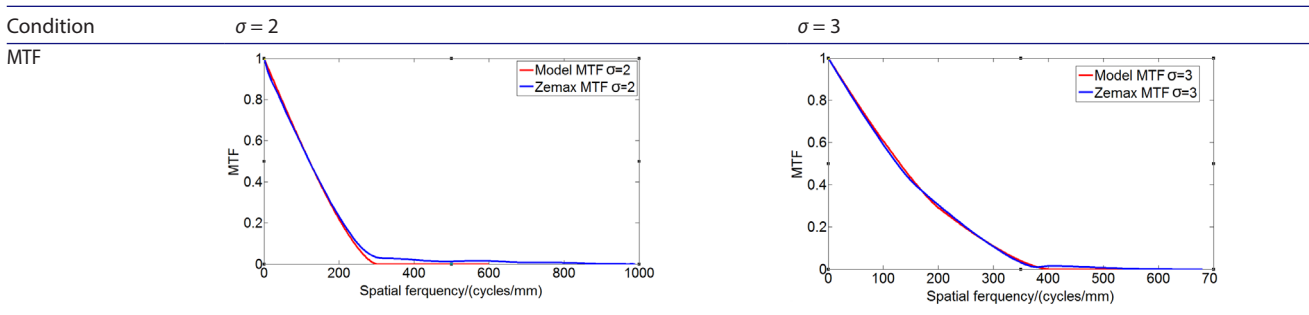


**Table 4.** The comparison of ZEMAX MTF and Model MTF when the system faces two equal window panes in different conditions in the polychromatic case.



0.3, we will need to make sure that  $MTF_{c}$  at the Nyquist frequency is greater than 0.54, according to Equation (27).

But, according to the Equation (20), when the phase difference is only related to the wedge angle of the pane, OTF includes a phase shift of  $e^{i2(n-1)\pi f_x \tan \gamma}$  which is dependent on  $f_x$  and  $\gamma$ . Even if the OTF is averaged over all wavelengths, the expressions of the OTF that include  $e^{i2(n-1)\pi f_x \tan \gamma}$  are not averaged to zero. The wedge angle of the pane has a great influence on the OTF. Based on the situation shown as Figure 16, taking  $\gamma = 0.00286^\circ$  as an example, Figure 17 shows the MTF of the Cassegrain system with the window by Equation (20). So, according to Equation (20), if design request  $MTF_{cw}$  at the Nyquist frequency is greater than 0.3, we will need to make sure that  $\gamma$  is less than  $0.001088^\circ$ , which provides referrals for tolerance analysis.

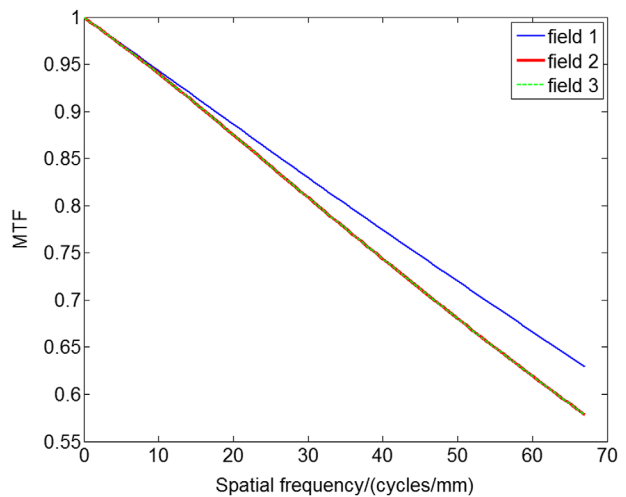


**Figure 14.** The MTF of the Cassegrain system.

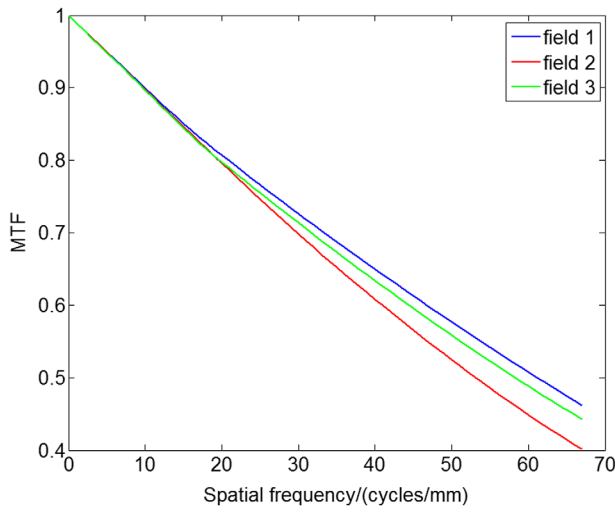


**Figure 15.** The MTF of the Cassegrain system with the window and  $\sigma = 3$ .

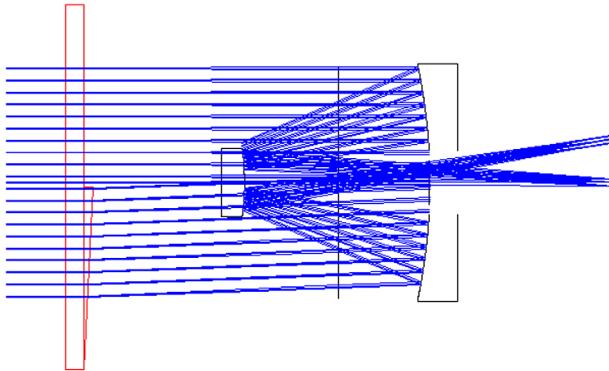


**Figure 16.** The model of the optical system aperture facing two panes with unequal thickness.

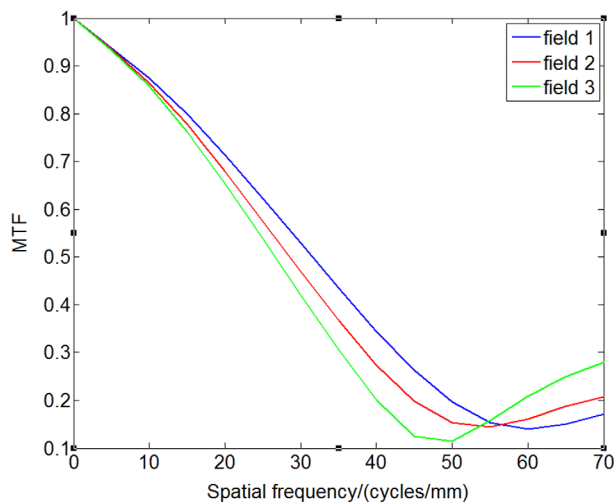


**Figure 17.** The MTF of the Cassegrain system with the unevenness window.

## 6. Conclusions

On the basis of above-mentioned MTF formulas, an optical system must simultaneously view through two or more panes of a mosaic window. There can be a serious loss in MTF over an appreciable range of spatial frequencies [2]. In the polychromatic case, the range and loss only depend on the position of the septa in the pupil and the non-parallelism of the panes. But in the monochromatic case, the range and loss also rely on the incidence angle. If the panes are tilted with respect to each other, then the loss must be accepted as there is no way to match optical thicknesses for all angles of incidence [2]. In summary, during use of the mosaic window in visible and infrared wavelengths and the process of product manufacture of the window, we should pay more attention to the pane precision and the configuration of the window. Meanwhile, we also should pay more attention to the incidence angle of the mosaic window used in monochromatic case. The formulas of the MTF also can be used to direct the design of optical system and provide reference to the machining and alignment. When the demands on MTF of the optical system with mosaic window are made, we can manipulate the formulas to get some technique data.

## Disclosure statement

No potential conflict of interest was reported by the authors.

## References

- (1) Hartmann, R. Airborne FLIR Optical Window Examples. Window & Dome Technologies & Materials III; **1992**. Proceedings of SPIE: Bellingham; vol. 1760; 1992; p. 86–96.
- (2) Gimlett, J. Modulation transfer function degradation in segmented windows. *Appl. Opt.* **1992**, *31*, 2981–2984.
- (3) Freiman, D. *Effect of Segmented Windows on the MTF of Optical Systems*. Meeting on Optical Engineering in Israel. International Society for Optics and Photonics, Proceedings of SPIE: Bellingham; vol. 2426; **1995**; pp. 399–408.
- (4) Friedman, M.; Vizgaitis, J. *Calculating Incoherent Diffraction MTF*. Infrared Imaging Systems: Design, Analysis, Modeling, and Testing XIX, Proceedings of SPIE: Bellingham; vol. 6941 (Suppl 36); **2008**; pp. 321–324.
- (5) Fischer, R.E.; Siegel, L.R.; Korniski, R.J. *New Developments in Optical Correction for Non-spherical Windows and Domes*. Window & Dome Technologies & Materials IV, Proceedings of SPIE: Bellingham; vol. 2286; **1994**; pp. 471–479.
- (6) Jones, M.I.; Jones, M.S. *Optical Analysis of Segmented Aircraft Windows*. Tactical Infrared Systems, Proceedings of SPIE: Bellingham; vol. 1498; **1991**; pp. 110–127.
- (7) Goorskey, D.J.; Drye, R.; Whiteley, M.R. Dynamic Modal Analysis of Transonic Airborne Aero-optics Laboratory Conformal Window Flight-test Aero-optics. *Opt Eng* **2013**, *52*, 2131–2139.
- (8) Chun, S.; Baek, W.; La, J. A Study on HILS for Performance Analysis of Airborne EOTS for Aircraft. *Journal of the Korea Society of Computer & Information* **2013**, *18*, 55–64.